Ignition of Gaseous Methane/Oxygen Coaxial Mixtures

C. Pauly and J. Sender
Deutsches Zentrum für Luft- und Raumfahrt
Raumfahrtantriebe
74239 Hardthausen, Deutschland

Abstract

Studies on the ignition and flame anchoring of a coaxial gaseous methane-oxygen jet have been performed. The experiment has been set up to record by high-speed visualization techniques the start-up and ignition transients. Results from image processing and data recording are evaluated for correlation of injection and stationary combustion conditions. The capability to perform reliable ignition of a gaseous methane/oxygen jet has been highlighted. Several phases of ignition ("expanding" and "stabilizing") have been found with specific phenomenology, depending mainly on the ignition time. The influence of the mass flow rate in terms of the J number on ignition process is discussed.

1. Introduction

For many years, the ignition phenomenon has been a crucial issue for the liquid propellant rocket engines. During the Ariane flights V15 and V18, deficiencies appeared in the reliability and the quality of ignition of the upper stage cryogenic HM7B engine, and are the cause of these failed flights. Moreover the actual multiple payload capability of the new Ariane launcher forces the upper stage engine to guarantee more than only one starting sequence, that means to ensure a reproducible, safe and reliable ignition, without blow down of the flame and without overpressure. Empirical methods are still the only reliable way to get understanding on such transient ignition. Modelling of reactive two phase flows under transient conditions is nowadays still challenging and confidence in the predictability of models and numerical simulations is still limited. However to improve the capability of CFD code to simulate such problems, several studies have already been performed to address these transient ignition phenomena ([1] - [6]). An ignition campaign with one-phase flow propellants (gaseous) has been already performed in M3 test facility [1], [5]. Such experiments can provide detailed data to be compared with numerical simulation and thus allow an improvement of the numerical tools.
The couple hydrogen/oxygen has a chemical reaction which is the most energetic producer and the combustion product is only water. However, the limitations imposed by the liquid hydrogen are more in producing, handling and storing operations. As alternatives the best performing non-toxic propellants have been found among hydrocarbons and in particular they are methane, propane and kerosene. These candidates present several advantages like higher density or easier storability at ambient conditions (lower cooling efforts). Several studies have shown that [despite their known tendency to produce soot reducing the ISP and a carbon layer at the cooling channel wall, which lowers the cooling efficiency], methane appears to be one of the best candidate [7].
This study presents the results of the GCHO test campaign, dedicated to study the ignition of a gaseous methane/oxygen jet. The focus is not only on the ignition and the flame stabilization processes of a methane/oxygen jet but also to provide detailed data to be simulated by CFD computations.

2. Experimental Set-Up

2.1. Combustion Chamber

The experimental test bench M3 Micro-combustor is composed of a horizontally mounted combustion chamber (CC). The section of the combustion chamber is rectangular and is composed of wide optical quartz windows which provide a complete optical access to the combustion chamber. Small windows located in the upper part of the chamber are

used to allow the access of the converged laser beam to the chamber (See 2.2). The dimensions of the chamber are given on the following figure: 60 x 60 x 140 mm.
The combustion chamber is equipped with a single coaxial injector. The injector has a simple geometry without recess and without tapering. The inner diameter of the oxygen diameter can be varied in order to achieve different injection conditions. The outer diameter of methane can also be varied for the same reasons (See Table 1).
Different nozzles geometries at the exit of the chamber can also be chosen in order to fix the total mass flow rate. The dome geometry is given hereafter (See Fig. 1).

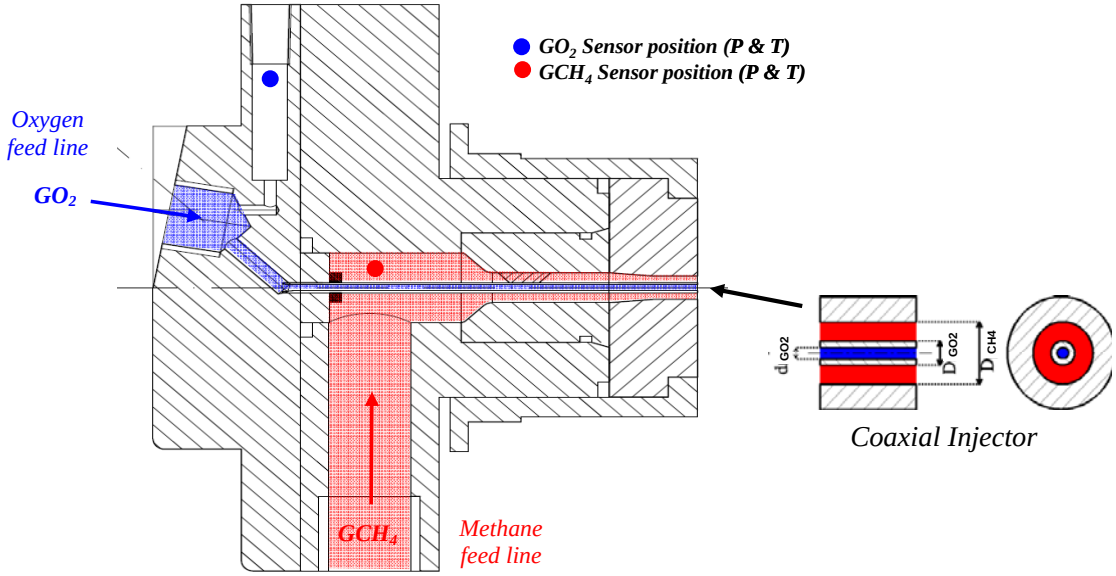

Fig. 1: Dome geometry of the methane/oxygen injector

2.2. Laser ignition

The ignition system is provided by a Nd-YAG Laser at 532 nm laser set up. The laser beam of 150mJ per pulse and a pulse length of 10 ns is focused inside the chamber creating induced plasma directly in the flow (see Fig. 2). The minimum breakdown energy deposition is for a methane/air mixture of 12 mJ [6] .
Though this ignition type is less representative than with a pyrotechnic igniter, it has real advantages in terms of precision of the spatial position and exact control of the ignition time. The data recording of both the optical diagnostics and sensors can be very precisely synchronized with the igniting laser pulse (precision of +/- 10 µs). The location of the ignition was set to 31 mm downstream the injector plate and 1 mm off jet axis. The approximated size of the induced plasma has been determinated from OH imaging and Schlieren as:

dX_{plasma} = 2.25 mm +/- 0.25 mm
dY_{plasma} = 3.4 mm +/- 0.4 mm

A more in depth description of the laser triggering is given in [3].

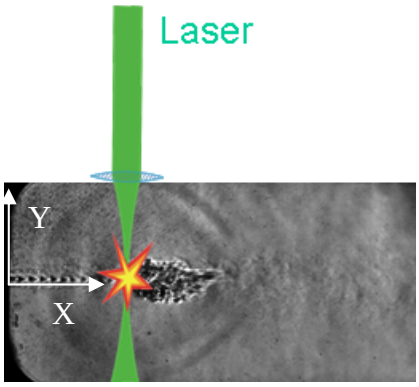

Fig. 2: Laser beam focused inside the chamber

2.3. Optical diagnostic systems

A standard Z-Schlieren was set-up with two different zoom settings, recording the images with a high speed CCD video camera at 2000 fps and with a resolution of 512 x 256 pixel. For test cases A and B an image region of 40 mm x 80 mm positioned directly at the injector exit was chosen to have a better resolution in this region. Test case C and D

are recorded using a lesser magnification giving a window size of 60 mm x 110 mm. An example for the latter can be seen in Fig. 2.
Additionally the spontaneous emission of intermittently existing OH-radicals is recorded by an intensified high speed CCD video camera. In this case the complete combustion chamber is visualized with a resolution of *512 x 256* pixels and a frame rate of 12500 fps. A band-pass filter (310 nm ± 5 nm) is used to select only the emission of the OH-radical.
The recorded OH emission images have been post-processed using image processing tools. A false colorization of the black and white images was applied in order to get a better visualization of the intensity gradient. In using a threshold value on the gray levels of the image, a detection of the flame front is realized. Calculated average images during steady combustion are used to determine the final lift-off distance of the flame. Figure 3 illustrates the image processing steps.

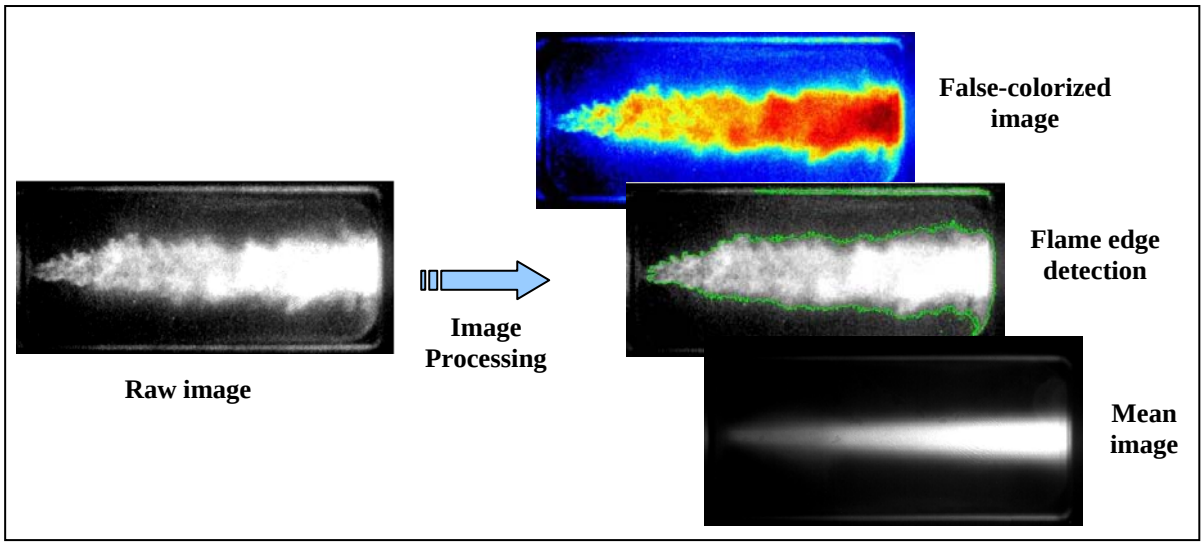

Fig. 3: Image Processing performed on OH images

2.4. Test time sequence

The chamber is continuously purged with nitrogen until 3000 ms before ignition time, so that it can be considered as completely filled with nitrogen. The fuel valve is opened 40 ms before the oxidizer in order to have fuel rich mixture at the ignition time. The hot flow run was finished one second after the ignition.
After stationary flow conditions in the injector dome are reached (80 ms for methane and 50 ms for oxygen after the first rise of each dome pressure sensor occurs) ignition is triggered.

2.5. Test conditions

Four test cases have been performed in modifying the geometrical characteristics of the injector (see Table 1). Test case A with an oxygen injector diameter of 1,6 mm was chosen for comparison with a precedent test case with GH2/GOx. However during the test, no attached flame was observed with this configuration.
Test cases B through D have been set up with an enlarged diameter to reduce the oxygen injection velocity. With this configuration, three different hydrogen slid widths were used to study the influence of the methane velocity.
With test case C the influence of the mass flow rate was studied using two different combustion chamber nozzles of 4 mm and 6 mm diameter respectively. The global geometrical characteristics and injection conditions are summarized in Table 1.

Table 1: Characteristics of injection

Test case	d_{GO2}	D_{GO2}	D_{CH4}	$D_{CC\ nozzle}$	p_{cc}	m_{tot}	v_{CH4}	v_{O2}	J	V_{ratio}
	[mm]	[mm]	[mm]	[mm]	[bar]	[g/s]	[m/s]	[m/s]	[-]	[-]
Case A	1.6	2.4	4.0	6	1.5	3.1	133	304	0.02	0.33
Case B	2.5	3.3	4.3	6	1.5 – 3.6	3.1 – 5.9	212-359	295	0.13	0.54
Case C1	2.5	3.3	3.6	6	2.3	4.6	424	305	1.53	1.72
Case C2	2.5	3.3	3.6	4	2.3	2.1	351	201	1.56	1.74
Case D	2.5	3.3	4.0	6	2.3	4.6	368	302	0.30	0.81

3. General Ignition Phenomenology

3.1. General Remarks

Based on the evaluation of the OH- and Schlieren-imaging the existence of three different possible ignition phases has been observed. These are, in order of appearance, a blown-down phase, an expansion phase (where the flame increases in size and intensity) and a stabilization phase.
However, an important factor determining how prominent each phase is represented, is the time delay between opening of the propellant valves and the laser pulse. Extending this delay increases the mass of unburnt gases in the CC resulting in higher pressure peaks at ignition and leading to a direct expansion without a blow down of the initial flame kernel (Figure 4). Figure 5 depicts such an explosive ignition, where the images are displayed for time intervals of 48 µs and 0.5 ms for OH and Schlieren imaging respectively.

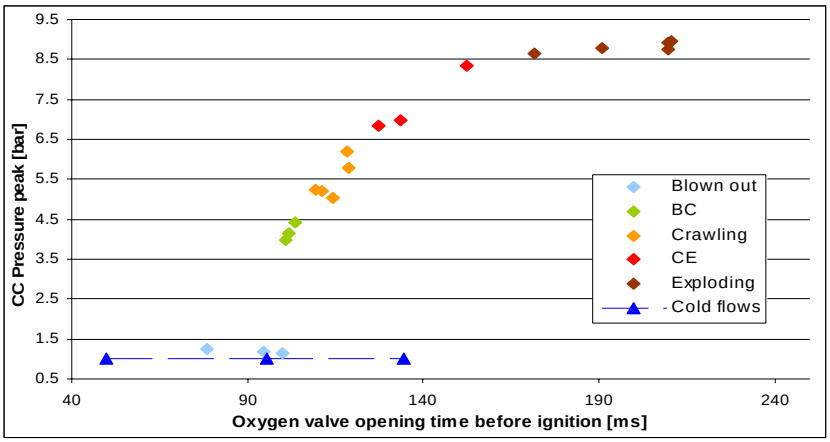

Fig. 4: Ignition type dependency with respect to the opening time

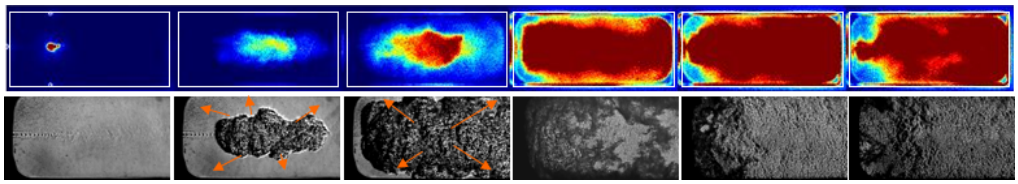

Fig. 5: OH and Schlieren images of expansion phase (0 - 2.5 ms)

3.2. Blow down phase

During this first possible phase, the flame is blown down towards the exit nozzle just after ignition and extinguishes. This occurs due to a small flame front velocity when compared to the propellant injection velocities.

3.3. Expansion phase

During the blow down phase in most cases hot gas expands, depending on the accumulated gases before ignition, more or less rapidly. This expansion continues on into the so-called expansion phase and occurs both in the upstream and downstream directions. The hot gases moving in the downstream direction are reflected and recirculate and realign along the central propellant jet. The mixing of these hot gases with the unburnt and colder propellants leads to a reignition. The location of reignition is variable.
In case of a prominent pressure peak, the feedlines are chocked, the flame extinguishes and is blown out. This pressure peak can also be observed in the dome pressure readings, indicating that a backflow of hot gases into the injector has occurred. This is supported by an analysis of OH emission images where a reignition in proximity of the injector exit is observable.

3.4. Stabilization phase

The last phase consists of the development and stabilization of the flame, which results in either a lifted or attached flame.
For the attached flame stabilization the typical behaviour of the upstream flame front, derived from OH emission recordings, is shown in Figure 6. After the aforementioned blow down the flame in one case is nearly extinguished, when it reignites at a position several diameters downstream the injector. From there the flame base moves slowly towards the injector and finally anchors there. At the injector exit the oxygen flow changes from sonic to subsonic condition during the ignition: at around 3 ms the expansion waves are no longer visible in the Schlieren images.

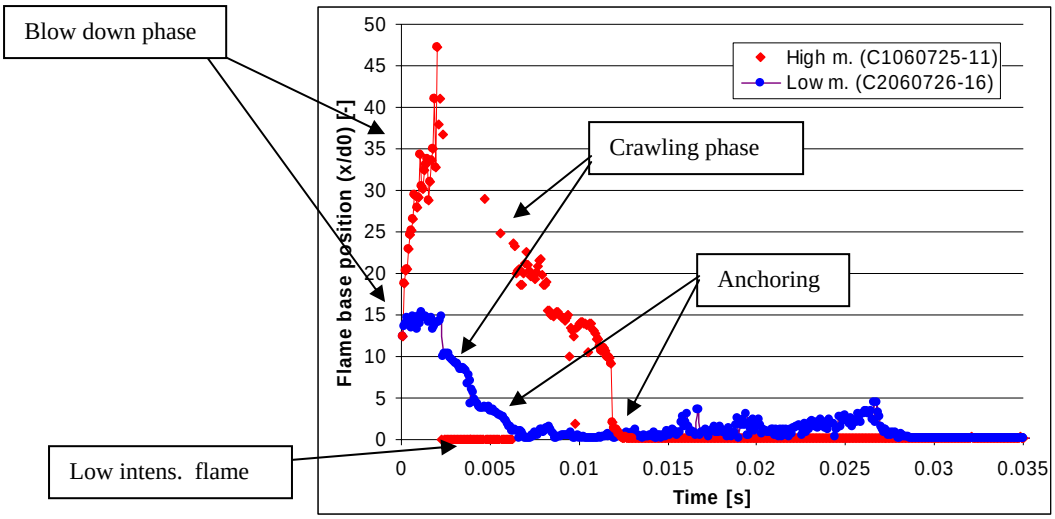

Fig. 6: Flame base position for attached flames with different mass fluxes

The lifted flame is after the blow down and expansion firstly attached to the injector. But when the initial pressure peak is released the flame base starts to lift off. Finally the flame base stabilizes fluctuating around a position 50 times the inner oxygen diameter (the end of the chamber is at 87 times the inner diameter) downstream the injector. These low frequency oscillations (ca. 100 Hz) couple with the feed lines and thus are also visible as OH emission intensity variations. Figure 7 shows an example of those oscillating OH emission intensity.

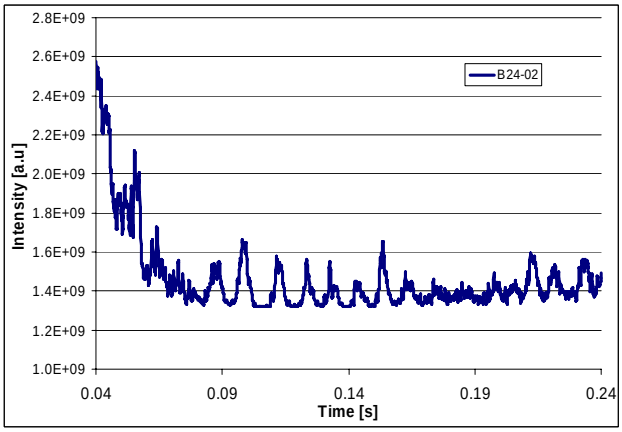

Fig. 7: LF oscillations of combustion: intensity and lift off distance

The shape of the flame is very different between the two flames. The attached flame is recognized by its pencil shape and with the maximum of OH emission quite downstream. The lifted flame is parabolic in shape and exhibits maximum intensity near its origin.

4. Influencing the Flame Stabilization

Figure 8 shows the flame mean images at stabilization phase for all different injection configurations. The images are averaged OH emission images during time period between 40 and 120 ms after ignition. The images are aligned with decreasing lift off distance, the left column is supplemented with Abel transformations of the mean images (top of the flame with colorization) to illustrate the contour of the flame in the median plan . On the right side table 5 shows for each configuration the corresponding momentum flux ratio J and velocity ratio V_{ratio} , defined as

$$J = \frac{\rho_{CH4} u_{CH4}^2}{\rho_{O2} u_{O2}^2} \quad (1)$$

$$V_{ratio} = \frac{u_{CH4}}{u_{O2}} \quad (2)$$

It can be clearly seen that for low values of velocity ratio and J number, the flame stays at a quite important distance from the injector lips (more than 15 times the injector diameter). Starting from a critical value of J number or velocity ratio the flame becomes stable. For low values of J number, the flame presents a round shape with a combustion maximum at the head of the flame. With increasing velocity ratios, the distance from the injector plate decreases and the shape of the flame changes to a pencil like shape where the maximal of OH radical emission is first at a downstream position and with much higher J number value, moves to an upstream position with a higher flame angle. Figure 9 shows this correlation more clearly.

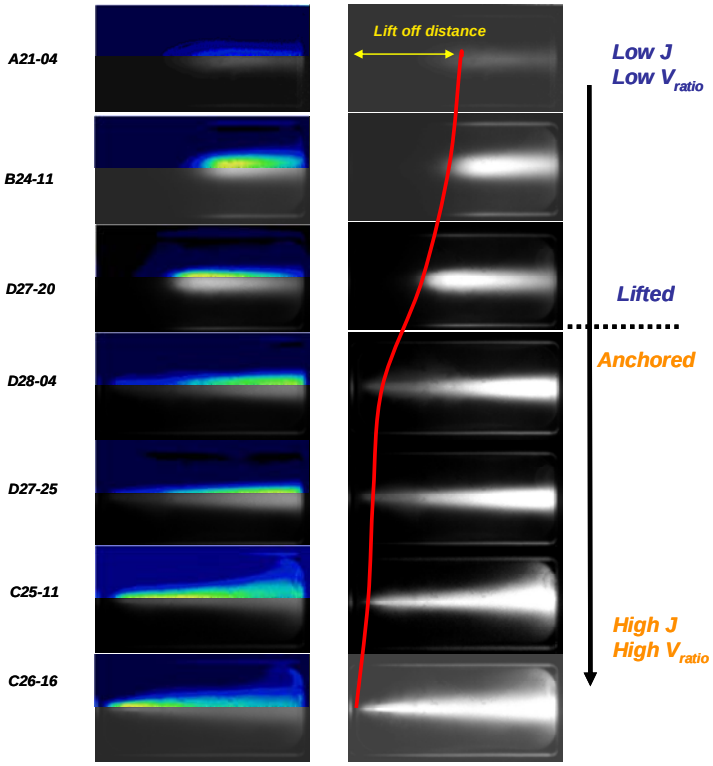

Fig. 8: Lifted and anchored flames

Test case	J [-]	V_{ratio} [-]
A21-04	0.017	0.32
B24-11	0.134	0.54
D27-20	0.256	0.754
D28-04	0.292	0.802
D27-25	0.321	0.845
C1-25-11	1.72	1.52
C2-26-16	1.77	1.59

Table 2: J and V_{ratio} for all test cases

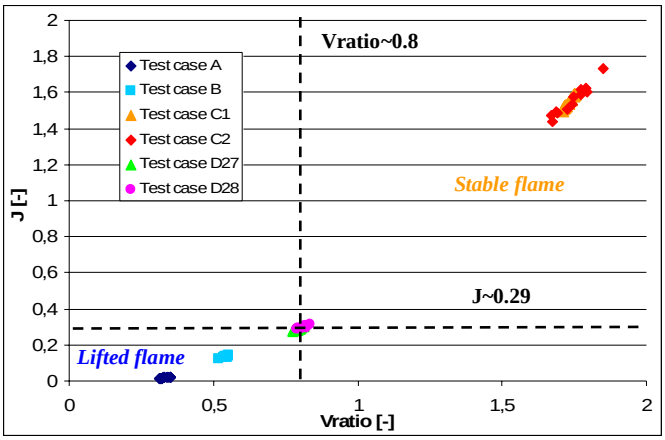

Fig. 9: Tests with stable and lifted flame

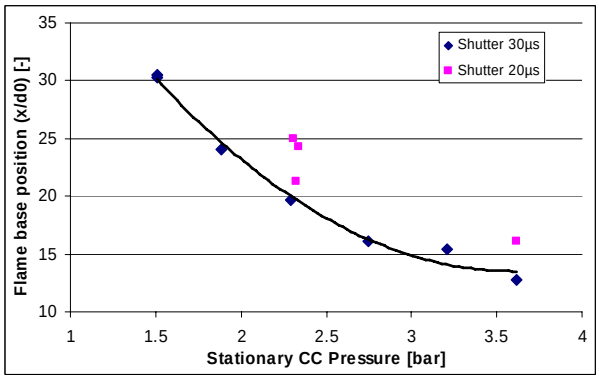

Fig. 10: Lift off distance for different P_c

The dependency of the flame stabilization on the CC pressure has also been analyzed. The only influence that could be found was for lifted flames of test case B. The CC pressure was varied from 1.5 bar to 3.62 bar. An average of image during the steady combustion is performed from 500 to 6000 images. The analysis showed that the CC pressure seems to favour the stabilization of the flame and reduce the lift off distance. Figure 10 shows the lift off distance of the mean image with respect to CC pressure. The lift off distance decreases from 30 times the inner oxygen diameter to 15 times with increasing CC pressure. Previous results show the same tendency when using GH_2/LO_X sprays [4].

5. Summary and Conclusions

During this campaign, the capability to perform reliable ignition of a gaseous methane/oxygen jet has been highlighted. Several phases of ignition have been found with specific phenomenology. For the different injector geometries used during this campaign, the CC pressure peak appears to be highly influenced by the valve opening times. The earlier the valves are opened, the stronger is the ignition process, because of a higher injected mass before ignition.
The CC pressure during steady state is certainly a parameter to stabilize the flame near the injector. An increase of the CC pressure decreases the lift-off distance of the lifted flame.
The influence of the J number and the velocity ratio on the ignition process has been highlighted. For the current test series stable and attached flames with a pencil like shape have been achieved within the region, which is limited by $J > 0.29$ and $V_{ratio} > 0.8$. Below that region lifted flames were observed, which show an inverse dependency of lift off distance to CC pressure. However high velocity ratios tested in case C required very small outer methane slit widths. Due to manufacturing uncertainties this led to asymmetries in the injector hardware and in turn to asymmetric injection conditions. For this reason test case series D are suggested as a reliable test case for further CFD simulation. It presents a reliable ignition process with good reproducibility, without asymmetries in injection and with a stable anchored flame during steady state combustion. The mass flow rates injected through the sonic nozzles are fixed during the entire duration of the test, providing reliable data concerning the boundary conditions of a CFD simulation.

Acknowledgement

The work was performed within the 'Long-Term Advanced Propulsion Concepts and Technologies' project investigating high-speed air breathing propulsion. LAPCAT, coordinated by ESA-ESTEC, is supported by the EU within the 6th Framework Programme Priority 1.4, Aeronautic and Space, Contract no.: AST4-CT-2005-012282. Further info on LAPCAT can be found on http://www.esa.int/techresources/lapcat. ESA-ESTEC is acknowledged for the internal research fellowship granted enabling the present research work.

References

[1] F. Cuoco, B. Yang, C. Bruno, O.J. Haidn, M. Oschwald, *Experimental investigation on LOX/CH4 Ignition*, AIAA 40th Joint Propulsion Conference, July 11-14 2004, Florida
[2] D. Preclik, P. Spagna, *Low Frequency and high frequency combustion oscillation phenomena inside a combustion chamber fed by liquid or gaseous propellants*, 1989
[3] V. Schmidt, U. Wepler, O.J. Haidn, M. Oschwald, *Characterization of the Primary Ignition Process of a coaxial GH2/Lox Spray*, AIAA 2004-1167
[4] V. Schmidt , D. Klimenko, O.J. Haidn, M. Oschwald, *Experimental Investigation and Modelling of Ignition Transient of a Coaxial H2/O2 Injector*, 5th International Symposium on Liquid Space Propulsion, Oct. 28-30 2003
[5] F. Cuoco, B. Yang, M. Oschwald, *Experimental Investigation of LOX/H2 and LOX/CH4 Coaxial Sprays and Flames*, 24th International Symposium on Space Technology and Science
[6] M. Weinrotter, B. Schwecherl, H. Kopecek, E. Wintner, *Laser Ignition of Methane-Air Mixture at High Pressures and Temperatures*
[7] A. Götz, C. Mäding, L. Brummer, D. Haeseler, *Application of non toxic propellants for future Advanced Launcher Vehicles*., 37th AIAA/ASME/SAE/ASEE, July 2001

A revised version of this article is availabe here.